

# Quasi-Elastic Scattering in MINERvA

Kevin S. McFarland

*Department of Physics and Astronomy, University of Rochester, Rochester, NY 14627 USA  
and Fermi National Accelerator Laboratory, Batavia, IL 60510 USA*

On behalf of the MINERvA Collaboration<sup>1</sup>

**Abstract.** Determination of the quasi-elastic scattering cross-section over a broad range of neutrino energies, nuclear targets and  $Q^2$  is a primary goal of the MINERvA experiment. We present preliminary comparisons of data and simulation in a sample rich in  $\bar{\nu}_\mu p \rightarrow \mu^+ n$  events from approximately one eighth of the total  $\bar{\nu}$  events collected by MINERvA to date. We discuss future plans for quasi-elastic analyses in MINERvA.

**Keywords:** Neutrino Interactions, Quasi-Elastic Scattering, Anti-neutrino

**PACS:** 13.15.+g,25.30.Pt,13.60.Fz

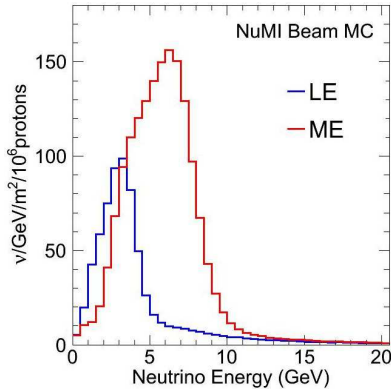
The MINERvA experiment was designed, in part, to study charged-current quasi-elastic (CCQE) neutrino ( $\nu_\mu n \rightarrow \mu^- p$ ) and anti-neutrino ( $\bar{\nu}_\mu p \rightarrow \mu^+ n$ ) scattering of neutrinos with energy 1 to 10 or more GeV over a broad range of  $Q^2$ . MINERvA is currently running in the "low energy" (LE) NuMI beam designed for the MINOS experiment in which it plans to integrate  $4 \times 10^{20}$  protons on target (POT) in neutrino mode and  $2 \times 10^{20}$  POT in anti-neutrino mode. The anti-neutrino exposure is a mixture of data taken with a partially constructed detector and the full MINERvA detector. After a shutdown beginning in 2012, the NuMI beamline will operate in the "medium energy" (ME) tune. Figure 1 shows the predicted neutrino flux in both the LE and ME beams.

The active elements of the MINERvA detector [1] are polystyrene scintillator bars formed into detector planes. A continuous series of these planes forms the "tracker" region of the MINERvA detector. The analysis reported in this paper used events exclusively from the tracker; however, the MINERvA detector also contains a region where the planes of scintillator are interspersed with passive nuclear targets. These will allow study of  $A$ -dependence in the CCQE rates at different energy or  $Q^2$ . Figure 1 also shows the expected rate of CCQE interactions in the scintillator tracker and in the passive nuclear targets. Of course, not all of these events will be accepted in the analysis, but the combination of the significant mass of the MINERvA targets and the high intensity statistics available in the NuMI beam are very promising for this measurement.

The planned results for CCQE in MINERvA include measurements of the CCQE total cross-section,  $\sigma$ , and  $d\sigma/dQ^2$  on the scintillator target. At low to moderate  $Q^2$ ,  $Q^2 \lesssim 1 \text{ GeV}^2$ , the primary goal is comparison with results from K2K [2, 3], MiniBoone [4, 5], SciBooNE [6] and NOMAD [7]. In particular, there are open questions about the apparent cross-section enhancement at low energy and moderate  $Q^2$  and suppression at

---

<sup>1</sup> <http://minerva.fnal.gov>



Interactions per $1.2 \times 10^{20}$ POT			
Target	LE $\nu_\mu$	LE $\bar{\nu}_\mu$	Mass
Scint. (CH)	58.0K	34.1K	6.4t
Helium	2.6K	1.3K	0.25t
Graphite (C)	1.5K	0.8K	0.17t
Water (H <sub>2</sub> O)	3.2K	2.2K	0.4t
Steel (Fe)	9.5K	4.3K	0.97t
Lead	11.4K	3.7K	0.98t

**FIGURE 1.** (left) The Neutrino Flux in the NuMI Low Energy (LE) and Medium Energy (ME) beams. Current MINERvA data is from the LE configuration, and future running concurrent with the NOvA experiment will use a spectrum more similar to the ME beam. (right) Fiducial CCQE Interactions in the Low Energy (LE) beam. The fiducial mass is also given in metric tons for each target.

low  $Q^2$  in the existing data. MINERvA will repeat these measurements on its multiple nuclear targets to look for changes with increasing  $A$  and nuclear density. At higher  $Q^2$ , MINERvA will be able to make the first measurements of the axial form factor and compare the high  $Q^2$  behavior with vector form factors. MINERvA also plans to compare  $\nu_e$  CCQE with the same  $\nu_\mu$  process using the  $\sim 1.5\%$  of its events from  $\nu_e$  contamination in the beam. Finally, MINERvA will search for the analogous neutral current process  $\nu p \rightarrow \nu p$  which is experimentally more challenging due to backgrounds from non-leptonic processes.

The study described in this paper is a preliminary comparison of muon kinematics in CCQE candidates between data and simulation with a sample of  $0.4 \times 10^{20}$  POT in the LE anti-neutrino beam. These data were taken during the construction of the MINERvA detector when only approximately one half of the detector had been installed. The scintillator tracker fiducial mass for this sample is 3.0 of the 6.4 metric ton fiducial mass available in the full detector. This sample is 12% of the total exposure measured as the product of POT and fiducial mass. The reference simulation is GENIE 2.6.2 [8]. The CCQE cross-section at nucleon level comes from the derivation of Llewellyn-Smith [9] with vector form factors from the BBBA2005 parametrization [10], the pseudo-scalar form factor from PCAC, and the axial form factor in the dipole form with  $m_A = 0.99 \text{ GeV}/c^2$ . The nuclear effects when scattering from carbon come from the Fermi gas model of Bodek and Ritchie [11], and Pauli blocking is implemented by a requirement that the outgoing nucleon has momentum of above the Fermi momentum of 221 MeV/c. Final state interactions of outgoing hadrons from the hard scattering process is simulated by INTRANUKE [8].

## SELECTION OF CCQE CANDIDATES

There are many possible approaches to the selection of CCQE candidates in the MINERvA detector. We expect, eventually, to have at least three strategies for selection, each

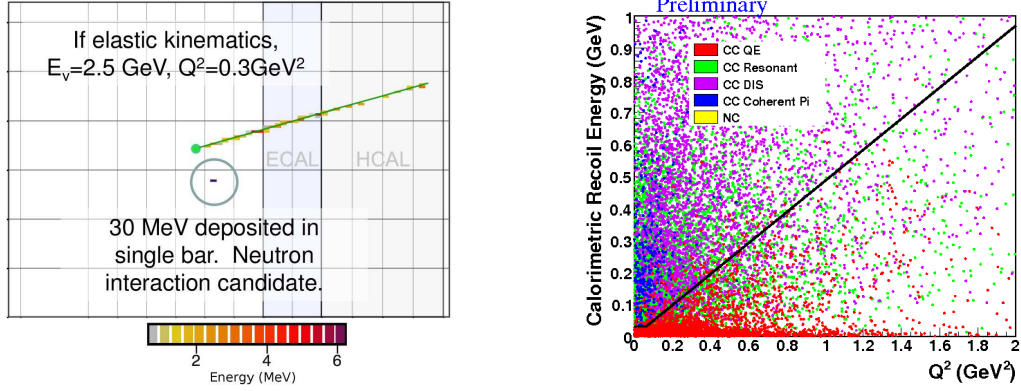


**FIGURE 2.** (left) A candidate event in the search for  $\bar{\nu}_\mu p \rightarrow \mu^+ n$ . The track originates in the scintillator region and is momentum analyzed in the MINOS near detector. The 30 MeV energy deposit away from the track is consistent with the direction of the recoil neutron. (right) For simulated events, the recoil energy away from the vertex vs.  $Q^2$  derived from the muon energy and angle. The region selected in this space keeps very high efficiency but lets in significant background at high  $Q^2$ .

of which will select different CCQE-rich final states and admit different backgrounds in the analysis. First, we can perform a topological track based analysis with a one-track (muon) low  $Q^2$  component and a two-track (muon and nucleon) component at higher  $Q^2$  where reconstruction of the nucleon, at least when it is a proton, is feasible. This style of analysis can be most easily compared to results using similar techniques from SciBooNE [6] and NOMAD [7]. Second, we can perform an inclusive analysis that selects only a muon and removes background based on a veto on Michel electrons from the chain  $\pi^+ \rightarrow \mu^+ \nu_\mu \rightarrow e^+ \nu_e \bar{\nu}_\mu \nu_\mu$  which is most similar to the analysis from the MiniBooNE [4, 5] experiment. Finally, one can identify tracks as in the first analysis but remove events with additional visible recoil energy in the detector which is far from the vertex. The latter stipulation is important for keeping events with low energy nucleons in the final state from the remaining nucleus after the CCQE interaction. The analysis presented here as our first preliminary work towards this reaction is in the final of these three styles. As we progress in this analysis, we plan to add the other techniques.

This analysis first selects events with a  $\mu^+$  originating from the scintillator tracker whose momentum and charge are measured in the MINOS near detector [1]. From the  $\mu^+$  reconstructed momentum and angle with respect to the neutrino beam direction we can reconstruct the neutrino energy and  $Q^2$ ,

$$E_\nu^{\text{rec}} = \frac{m_n^2 + 2E_\mu (m_p - E_B) - (m_p - E_B)^2 - m_\mu^2}{2 \left( m_p - E_B - E_\mu + \cos \theta_\mu \sqrt{E_\mu^2 - m_\mu^2} \right)} \quad (1)$$

$$\text{and } (Q^2)^{\text{rec}} = 2E_\nu^{\text{rec}} \left( E_\mu - \cos \theta_\mu \sqrt{E_\mu^2 - m_\mu^2} \right) - m_\mu^2, \quad (2)$$

where  $m_n$ ,  $m_p$  and  $m_\mu$  are the neutron, proton and muon masses,  $E_\mu$  and  $\theta_\mu$  are the muon energy and angle, and  $E_B$  is the target proton binding energy, 34 MeV in our estimation of the neutrino kinematics.

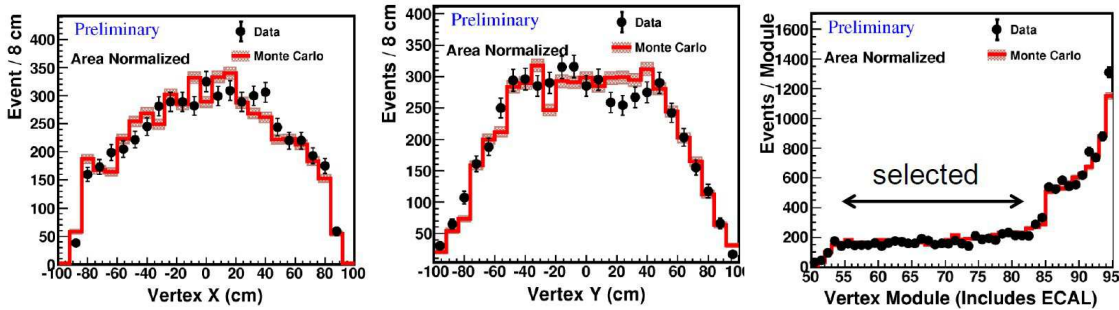


**FIGURE 3.** Distributions of the position at which the muon in  $\bar{\nu}_\mu p \rightarrow \mu^+ n$  originates. (left and middle) The transverse directions,  $x$  and  $y$  within the hexagonal fiducial volume. (right) The direction along the beam, including regions outside the fiducial volume selected by the analysis such as the more dense electromagnetic calorimeter (ECAL) region downstream of the fiducial volume and the very dense hadron calorimeter (HCAL) farther downstream.

A quasi-elastic candidate event passing this selection is shown in Fig. 2. The only other visible energy in the event is the single bar with a 30 MeV deposit consistent with the expected direction of recoil based on the direction and energy of the muon. The expected recoil is a neutron with kinetic energy of 150 MeV. Typically only a small fraction of the neutron energy is observed calorimetrically in the MINERvA detector.

For this first analysis, we chose a very conservative cut on the recoil energy in order to keep the efficiency of the analysis high. This approach, however, lets in significant backgrounds, particularly at high  $Q^2$  as shown in Fig. 2. For events originating within the fiducial volume, the asymptotic efficiency at high energies is  $\approx 65\%$ . The efficiency is highest at low  $Q^2$  and falls slowly to  $\approx 30\%$  at high  $Q^2$  not because of the low recoil selection, but because of the decrease in muon acceptance to enter the MINOS near detector. A hit-level GEANT4-based simulation of the detector is used to evaluate these efficiencies and correct the neutrino interaction simulation for detector efficiencies and resolutions. We gain confidence in this simulation by comparison of distributions of candidate events in the data with the simulation in quantities that are largely independent of the neutrino flux and the interactions. For example, Fig. 3 shows that the distribution of candidate vertices in the transverse and longitudinal dimensions of the detector agrees with a relatively normalized simulation.

## RESULTS

We present the results as comparisons to the simulation, including background events generated as described above. The simulation also includes our prediction of the untuned flux from a beamline simulation which has large uncertainties that we expect to reduce in the future [12]. We evaluate these uncertainties in the *a priori* neutrino flux to be lowest, about 7%, at the peak energy of the flux shown in Fig. 1 and significantly larger above this “focusing peak” energy with an asymptotic uncertainty at high energy of 16%. These large flux uncertainties must be included in the comparisons between data candidates and the simulation. These uncertainties allow a significant distortion in shape

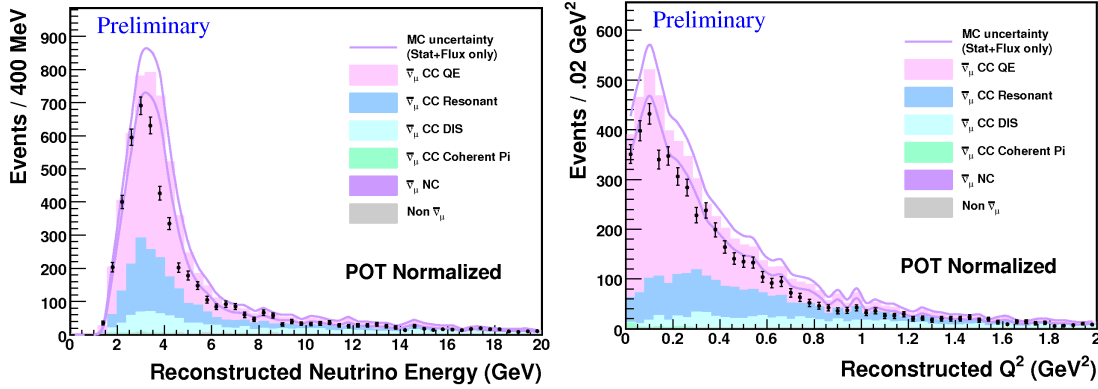


**FIGURE 4.**  $E_\nu$  (left) and  $Q^2$  (right) reconstructed from muon kinematics by Eqns. 1 and 2, respectively, for  $\bar{\nu}_\mu p \rightarrow \mu^+ n$  candidates. Different reactions in the simulated event sample are shown stacked in the solid histogram. The flux uncertainty is shown as a band around the simulation prediction.

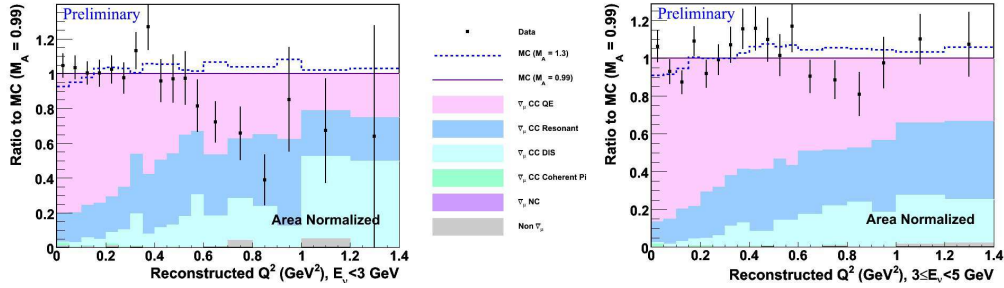


**FIGURE 5.** The relatively normalized ratio of data to simulated  $Q^2$  distributions for  $E_\nu < 3$  GeV (left) and  $3 < E_\nu < 5$  GeV (right). The uncertainties shown are statistical only; flux uncertainties approximately cancel in the analysis of the shape of this distribution, detector systematics and background uncertainties which are not included in the shown uncertainties may not. The change in shape expected if  $m_A = 1.3$  GeV is also shown.

of the neutrino flux with neutrino energy,  $E_\nu$ . However, since the  $Q^2$  spectrum as a function of  $E_\nu$  is approximately independent of  $E_\nu$ , at least far below the kinematic limit,  $Q^2 \lesssim 2m_p E_\nu$ , we do not expect the flux uncertainties to significantly distort the predicted  $Q^2$  distribution.

Figure 4 shows the reconstructed neutrino energy and  $Q^2$  of the reactions for candidate events. The comparison shows a disagreement outside the uncertainty band in the distribution of neutrino energies just above the focusing peak,  $3 \text{ GeV} < E_\nu < 6 \text{ GeV}$ . However, the shape of the  $Q^2$  distribution, at least in the region where CCQE events make up the majority of the signal, is in reasonable agreement with our simulation. Note that the simulation uses an axial mass of 0.99 GeV. MiniBooNE and SciBooNE, measuring quasi-elastic neutrino and anti-neutrino scattering for  $0.3 < E_\nu < 2 \text{ GeV}$ , prefer significantly higher axial masses, consistent with  $m_A = 1.3 \text{ GeV}$  [4, 5, 6], whereas the NOMAD experiment, measuring quasi-elastic neutrino scattering,  $3 < E_\nu < 100 \text{ GeV}$ , prefers  $m_A$  consistent with the value of 0.99 GeV assumed in our simulation. Figure 5 shows the ratio of data to simulation for the MINERvA analysis in the low and high

neutrino energy portions of the sample. Both appear more consistent with the low  $m_A$  assumed rather than the high  $m_A$  of MiniBooNE and SciBooNE; however, caution is warranted in drawing this conclusion because the MINERvA result only includes systematic uncertainties from the neutrino flux, and does not yet include uncertainties on the detector reconstruction or the backgrounds to the quasi-elastic interactions.

## CONCLUSIONS

The MINERvA collaboration has performed its first comparison of a quasi-elastic rich anti-neutrino sample with expectations for a range of assumed axial masses. The selection requires a muon from a neutrino interaction in the scintillator target and a low observed recoil away from the vertex in the final state to enhance elastic events. MINERvA possesses an anti-neutrino sample approximately eight times as large as that in this analysis on tape, and will be able to improve the background rejection of this analysis in the future through a variety of techniques that the capabilities of the detector make possible.

## ACKNOWLEDGMENTS

This work was supported by the Fermi National Accelerator Laboratory, which is operated by the Fermi Research Alliance, LLC, under contract No. DE-AC02-07CH11359, including the MINERvA construction project, with the United States Department of Energy. Construction support also was granted by the United States National Science Foundation under NSF Award PHY-0619727 and by the University of Rochester. Support for participating scientists was provided by NSF and DOE (USA) by CAPES and CNPq (Brazil), by CoNaCyT (Mexico), by CONICYT (Chile), by CONCYTEC, DGI-PUCP and IDI-UNI (Peru), and by Latin American Center for Physics (CLAF). Additional support came from Jeffress Memorial Trust (MK), and Research Corporation (EM). Finally, the authors are grateful to the staff of Fermilab for their contributions to this effort and to the MINOS collaboration for their efforts to operate the MINOS near detector and willingness to share its data.

## REFERENCES

1. D. Schmitz, “The MINERvA Neutrino Scattering Experiment”, these proceedings (2011).
2. R. Gran *et al.* [K2K Collaboration], Phys. Rev. **D74**, 052002 (2006).
3. X. Espinal and F. Sanchez [K2K Collaboration], AIP Conf. Proc. 967, 117 (2007).
4. A. A. Aguilar-Arevalo *et al.* [MiniBooNE Collaboration], Phys. Rev. Lett. **100**, 032301 (2008)
5. A. A. Aguilar-Arevalo *et al.* [MiniBooNE Collaboration], Phys. Rev. **D81** 092005 (2010).
6. J. L. Alcaraz-Aunión and J. Walding [SciBooNE Collaboration], AIP Conf. Proc. 1189, 145 (2009).
7. V. Lyubushkin *et al.* [NOMAD Collaboration], Eur. Phys. Jour. **C63**, 355 (2009).
8. C. Andreopoulos *et al.*, Nucl. Instrum. Meth. **A614** 87 (2010).
9. C. H. Llewellyn Smith, Phys. Rept. **3** 261 (1972).
10. A. Bodek, R. Bradford, H. Budd and J. Arrington, Nucl. Phys. Proc. Suppl. **159** 127 (2006).
11. A. Bodek and J. Ritchie, Phys. Rev. **D23** 1070 (1981).
12. M. Jerkins, “Measuring the NuMI Beam Flux for MINERvA”, these proceedings (2011).